

# Tradeoffs in Processing Queries and Supporting Updates over an ML-Enhanced R-tree

Abdullah-Al-Mamun, Ch. Md. Rakin Haider, Jianguo Wang, Walid G. Aref, *Fellow, IEEE*,

**Abstract**—Machine Learning (ML) techniques have been successfully applied to design various learned database index structures for both the one- and multi-dimensional spaces. Particularly, a class of traditional multi-dimensional indexes has been augmented with ML models to design ML-enhanced variants of their traditional counterparts. This paper focuses on the R-tree multi-dimensional index structure as it is widely used for indexing multi-dimensional data. The R-tree has been augmented with machine learning models to enhance the R-tree performance. The AI+R-tree is an ML-enhanced R-tree index structure that augments a traditional disk-based R-tree with an ML model to enhance the R-tree’s query processing performance, mainly, to avoid navigating the overlapping branches of the R-tree that do not yield query results, e.g., in the presence of high-overlap among the rectangles of the R-tree nodes. We investigate the empirical tradeoffs in processing dynamic query workloads and in supporting updates over the AI+R-tree. Particularly, we investigate the impact of the choice of ML models over the AI+R-tree query processing performance. Moreover, we present a case study of designing a custom loss function for a neural network model tailored to the query processing requirements of the AI+R-tree. Furthermore, we present the design tradeoffs for adopting various strategies for supporting dynamic inserts, updates, and deletes with the vision of realizing a mutable AI+R-tree. Experiments on real datasets demonstrate that the AI+R-tree can enhance the query processing performance of a traditional R-tree for high-overlap range queries by up to 5.4X while achieving up to 99% average query recall.

**Index Terms**—Machine Learning for Database Systems, Learned Indexes, Spatial Indexing, Query Processing

## I. INTRODUCTION

Recently, machine learning techniques (ML techniques, for short) have been successfully applied to build various learned database system components [1]. Particularly, ML techniques have been applied to database indexes to build learned index structures, e.g., [2]–[5] for the one-dimensional space. The concept of learned one-dimensional learned indexes has been extended to realize learned multi-dimensional indexes [6]–[10]. Moreover, learned indexes can be broadly categorized into two types: *Pure* and *Hybrid* learned indexes [10]. The core idea behind the class of hybrid learned indexes is that they incorporate ML models to enhance the performance of a traditional index structure [11], [12]. These hybrid learned indexes can also be viewed as ML-enhanced variants of their traditional counterparts.

On the other hand, traditional multi-dimensional (e.g., spatial) index structures have been used successfully over the years as efficient access methods for multi-dimensional data (e.g., location data). In the area of spatial databases, the R-tree [13] is a widely-used index structure. In the

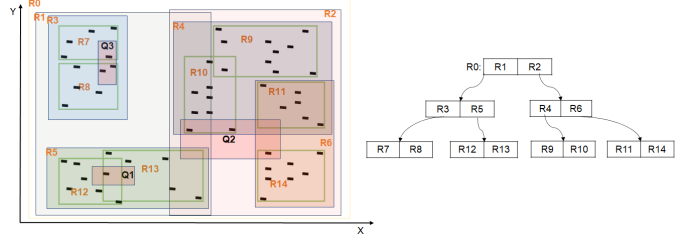


Fig. 1. An example of an R-tree with overlapping nodes

multi-dimensional space, the R-tree is analogous to the one-dimensional index structure B<sup>+</sup>-tree [14]. In the R-tree, objects are stored using Minimum Bounding Rectangles (MBRs). Notice that in the B<sup>+</sup>-tree, nodes do not overlap in space. However, the MBRs of non-leaf and leaf nodes of an R-tree can overlap in space.

In this paper, we focus on processing range queries over an R-tree due to their wide applicability in spatial databases [15]. Figure 1 illustrates the impact of node overlap in an R-tree to answer a range query. Notice that the number of accessed leaf nodes directly impacts the query response time of an R-tree [15]. For a disk-based R-tree, descending multiple paths in the R-tree incurs high I/O cost [16]. In Figure 1, the leaf nodes of the R-tree are labeled R7-R14. Consider Range Queries Q1, Q2, and Q3. For Q1, we search the R-tree down the 2 paths (from root to leaf):  $R1 \rightarrow R5 \rightarrow R12$  and  $R1 \rightarrow R5 \rightarrow R13$  while only the latter path contains actual query results. Hence, accessing the leaf node R12 is wasted. For Q2, we search the R-tree along 4 paths:  $R1 \rightarrow R5 \rightarrow R13$ ,  $R2 \rightarrow R4 \rightarrow R10$ ,  $R2 \rightarrow R6 \rightarrow R11$ , and  $R2 \rightarrow R6 \rightarrow R14$  while only the 2nd and 4th paths contain output data objects. Hence, accessing the leaf nodes R11 and R13 negatively impacts query processing performance. For Query Q3, the R-tree searches two paths:  $R1 \rightarrow R3 \rightarrow R7$  and  $R1 \rightarrow R3 \rightarrow R8$ , where both paths contain output data objects. In both Q1 and Q2, the R-tree accesses 50% more leaf nodes than the true number of leaf nodes containing the output data objects. In contrast, for Query Q3, the R-tree searches both R7 and R8, and data objects are exactly found in both nodes. In this case, the number of visited leaf nodes by the R-tree matches the true number of leaf nodes required to answer Q3. Thus, in terms of the number of leaf node accesses, we can identify Q1 and Q2 as high-overlap queries and Q3 as a low-overlap query. Observe that the R-tree searches extraneous leaf nodes to answer Q1 or Q2 but performs optimally for Q3. We define an overlap ratio  $\alpha$  to quantify the degree of extraneous leaf node accesses

required by a query. Specifically, for a range query, we divide

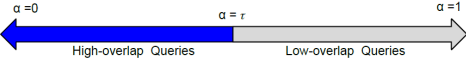


Fig. 2. Spectrum of the overlap ratio  $\alpha$  with Threshold  $\tau$  to identify high- and low-overlap queries

the number of true leaf nodes by the total number of visited leaf nodes to estimate  $\alpha$ , e.g., in Figure 1, to answer Q2, the number of visited leaf nodes is 4 while the number of true leaf nodes is 2 making  $\alpha = 0.50$ . Similarly, for Q1 and Q3,  $\alpha$  is 0.50 and 1, respectively. Notice that the number of true leaf nodes cannot exceed the number of visited leaf nodes. Hence,  $\alpha$  ranges from  $[0 - 1]$ .

For the purposes of this paper, the high- and low-overlap queries are determined as follows: Based on a pre-defined threshold  $\tau$ , queries with overlap ratio  $\alpha \leq \tau$  (i.e., closer to 0) are high-overlap while queries with  $\alpha > \tau$  (i.e., closer to 1) are low-overlap. The spectrum of the overlap ratio  $\alpha$  with Threshold  $\tau$  is given in Figure 2.

Motivated by the benefits of hybrid learned indexes and considering the issue of node overlap in the R-tree, the following important questions arise: *Which workloads degrade the performance of range query processing in a traditional R-tree? Can we leverage ML techniques to make R-tree range query processing faster?* Hence, we formulate the problem as follows: **Given a range query  $Q(X_{min}, Y_{min}, X_{max}, Y_{max})$ , we need to predict the true leaf nodes of the R-tree that contain output data objects, and only access these nodes without accessing extraneous ones.** In this paper, the proposed AI-tree transforms this problem into a multi-label classification [17] task by treating the leaf node IDs as the class labels. For example, classifying a research paper into a Systems, Theory, or ML paper is a multi-label classification task as a paper can be both a Systems and ML paper. Analogously, we can cast answering a range query over the R-tree as a multi-label classification task, where the classes are the R-tree leaf nodes, and we need to find these nodes that overlap the range query and that contain the output objects to the query. At query time, the trained multi-label classifier predicts the true leaf node IDs that contain data entries that fall inside the query region. Hence, with correct prediction, the AI-tree only needs to access the true leaf nodes (i.e., without accessing any extraneous nodes) to process the query. As a result, *the choice of ML models plays an important role in the query processing performance of the AI-tree [18].* Moreover, for leveraging the benefit of both a traditional R-tree and an ML-enhanced AI-tree, the hybrid AI+R-tree [18] has been proposed (refer to Figure 3). The AI+R-tree uses the overlap ratio  $\alpha$  to identify the high-overlap queries for which an R-tree accesses many extraneous leaf nodes. Here, the Overlap Ratio Classifier (a binary classifier [19]) routes the high-overlap queries to the AI-tree component and the low-overlap queries to the R-tree component. After that, the AI-tree and the R-tree process the high- and low-overlap queries, respectively. For an input query, if the AI-tree returns an empty result set (i.e., predicting all false positives/negatives), we call the regular R-tree to verify and resolve this case. Moreover, the

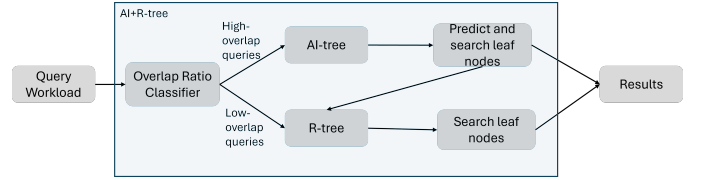


Fig. 3. The AI+R-tree

AI+R-tree indexes the learned models [20] as it uses a grid to decide which ML model to invoke from the multiple models that the AI-tree component has. For fixed query workloads, experiments on real spatial data demonstrate that the AI+R-tree significantly enhances the performance over a traditional R-tree.

This paper extends over the previous conference paper on the AI+R-tree [18], and makes the following new contributions:

- We extend the AI+R-tree to process dynamic query workloads, and present empirical tradeoffs in query processing by varying the choice of ML models. We adopt three performance metrics: Query Recall, Query Processing Time, and ML Model Size. Moreover, we include a case study of designing a custom loss function for a neural-network-based model tailored to the query processing requirements of the AI+R-tree.
- We present design tradeoffs to extend the immutable AI+R-tree to support dynamic data insert/update/delete with the vision of realizing a mutable AI+R-tree.
- For dynamic query workloads, experiments on real datasets demonstrate that the AI+R-tree can enhance query performance for high-overlap range queries by up to 5.4X while maintaining up to 99% recall.

The rest of this paper proceeds as follows: Section II provides an overview of the AI-tree. Section III presents the hybrid AI+R-tree. Section IV investigates the choice of ML models in the AI+R-tree. Section V presents design tradeoffs for supporting dynamic data inserts and updates. Section VI presents experimental results. Section VII discusses the related work. Section VIII provides several directions for future research. Finally, Section IX concludes the paper.

## II. THE AI-TREE

We overview the AI-tree with the extensions made to the training steps of the AI-tree to process dynamic query workloads.

### A. The Preprocessing Phase

1) *Assigning Unique Identifiers to the R-tree Leaf Nodes:* In the preprocessing step, each R-tree node is assigned a unique identifier (ID) based on Depth First Search (DFS) order.

2) *Definition (The Overlap Ratio  $\alpha$ ):* Given a range query, say  $Q$ , to calculate the value of  $\alpha$ , we use two metrics:  $TN(Q)$ , the true unumber of leaf-node accesses required to process  $Q$ , and  $VN(Q)$ , the unumber of leaf nodes visited by the R-tree

index to answer Q. For the range query Q, the definition of  $\alpha$  is as follows (the value of  $\alpha$  is in the interval  $[0, 1]$ ):

$$\alpha = \frac{TN(Q)}{VN(Q)}$$

3) *Query Workload Categorization*: Given a query workload, we categorize each query based on its selectivity. After identifying the selectivity of a query, the overlap ratio  $\alpha$  of the query is calculated to further categorize the queries based on their value of  $\alpha$ . This is achieved by executing the query during the preprocessing phase, computing the query’s selectivity, the leaf nodes being touched, and the true leaf nodes.

4) *Training Data and Features*: We prepare the training data following a two-step process. In the first step, all queries in the query workload are executed one at a time on the constructed R-tree over the given dataset. For each executed query, we collect the following information: The IDs of the leaf nodes that the R-tree visits to answer the query, and the true leaf node IDs that contain the output data objects that are actually inside the query region. Moreover, for an input range query Q, we use the values  $(X_{min}, Y_{min}, X_{max}, Y_{max})$  of the query rectangle as input features to the ML model without any additional transformation. Thus, the same input can be processed seamlessly by both the AI-tree and the R-tree. For multi-label classification, the output labels are encoded using one-hot encoding [21], where we represent the class labels using binary values.

### B. Learning the R-tree Index: ML Model Training and Testing

Refer to Figure 4. The workflow for training and testing the multi-label classifier is as follows. (1) While the given queries

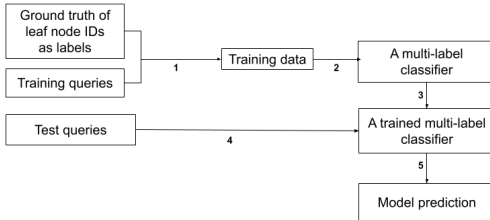


Fig. 4. Workflow of ML model training and testing

are executed by the R-tree, for each query, the IDs of the visited and true leaf nodes are captured. (2) Then, the training queries are used to train the multi-label classifier. *In this paper, the goal is to enhance the performance of the AI-tree for dynamic query workloads. As a result, the training queries are further divided into two sets: training and validation. ML models are trained on the training set and the hyperparameters are tuned based on the performance on the validation set.* (3) A trained multi-label classifier is created after the training phase. (4) The test queries are given as input to the trained multi-label classifier. (5) At query time, the pre-trained multi-label classifier is invoked to directly predict the true leaf node IDs that contain the query result.

### C. Indexing the Learned Models: A Multi-model Approach

The idea of indexing multiple learned models using a traditional index structure has been used in the context of handwritten and time series data [20]. In the AI-tree, we use a simple coarse grid structure to group the training queries. We train a separate ML model over queries inside each grid partition. The grid serves as an index to the localized learned ML models.

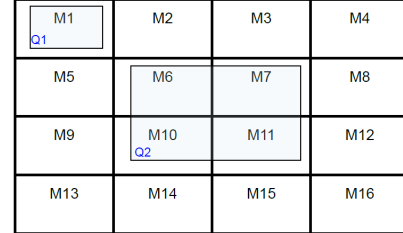


Fig. 5. Indexing the learned models

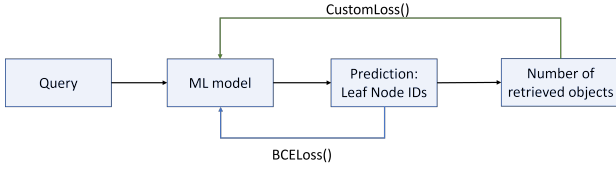
For example, in Figure 5, the space is partitioned using a 4X4 grid. In the training phase, we incrementally search for the grid size that produces the best fit over the validation set [22]. In Figure 5, as Query Q1 falls completely inside the top-left grid cell, only model M1 is trained for Q1. On the other hand, as Query Q2 overlaps four grid cells, the four models M6, M7, M10, and M11 are trained for Q2. If multiple models are trained for a particular query, during query processing, we aggregate their prediction results from all the overlapping cells.

## III. THE AI+R-TREE

To achieve the best of both the AI-tree and the R-tree, the hybrid AI+R-tree (see Figure 3) processes the high-overlap queries using the AI-tree and the low-overlap queries using the traditional R-tree. However, this is non-trivial because the overlap ratio  $\alpha$  of a query is unknown until we process the query. Hence, we leverage ML techniques to learn how to distinguish between high- and low-overlap queries. Specifically, the problem of classifying the range queries based on the value of  $\alpha$  and the threshold  $\tau$  can be formulated as a binary classification task [19]. To prepare the training data for a particular dataset, we combine the queries for each of the  $\alpha$  values. Then, we assign Label 0 for the queries whose  $\alpha$  value is less than or equal to the threshold  $\tau$ , and assign Label 1 for the queries whose  $\alpha$  value is greater than the threshold  $\tau$ . Next, a binary classifier is trained on the training queries. At query time, the pre-trained binary classifier (i.e., overlap ratio classifier) is invoked to classify an incoming range query into either a high- or a low-overlap query.

### A. Query Processing over the AI+R-tree

Given a range query, say Q, the binary classifier is invoked first (see Figure 3) to predict whether Q is high- or low-overlap. If Q is classified as a high-overlap query, the AI-tree processes the query. Otherwise, the R-tree processes the query. Notice that query processing using the AI+R-tree incurs a prediction cost before accessing the leaf nodes. Hence, the cost



(a) Workflow of the custom loss function

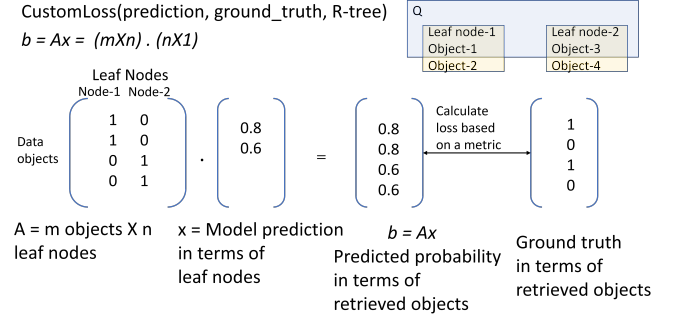
Fig. 6. Designing a custom loss function for the NN model

of query processing of the AI+R-tree is: ML model prediction cost + I/O cost. Thus, we expect to get the benefit of the AI-tree for processing the high-overlap queries whose  $\alpha$  value is closer to zero. On the other side of the spectrum of  $\alpha$  (Figure 2), for the queries with  $\alpha$  closer to one, the R-tree is expected to perform better than the AI-tree. For example, consider the three queries in Figure 1. For Queries Q1 and Q2, the overlap ratio  $\alpha = 0.50$ . If the AI+R-tree can accurately predict the leaf nodes, 50% less number of leaf nodes will be accessed to answer the query. Notice that there is room for improvement to process Q1 and Q2 using the AI-tree component of the AI+R-tree. In contrast, for Q3,  $\alpha = 1$ . Thus, both the visited leaf nodes contain data entries that fall inside the query rectangle. Thus, it is not possible for the AI-tree to process the query using less leaf node accesses than the R-tree. Thus, we use the R-tree component in this case.

1) *Query Processing using the AI-tree Component*: Given a range query, the ML models are identified whose grid cells overlap the range query. Then, only these models are executed to process the query. The resulting leaf node IDs from the ML model prediction are aggregated. Then, only the corresponding leaf nodes of these IDs are accessed. Finally, the data entries in these leaf nodes are checked against the input query rectangle, and only the ones actually contained are reported. This ensures that the AI-tree never returns a false-positive query result. However, for a given query, the AI-tree can produce query results with false negatives, which impacts query recall.

Notice that the AI-tree is expected to only access the predicted leaf nodes without accessing the extraneous leaf nodes. Thus, if the ML models inside the AI-tree predict the leaf nodes accurately, the minimum number of leaf nodes is accessed to answer a query. This reduces the number of disk I/Os for processing a range query. Notice further that for a given query, if the trained multi-label classifier mispredicts all leaf node IDs, the AI-tree returns an empty result set. This can happen either due to the misprediction of the ML models or the range query indeed returns an empty set if processed by the R-tree. As a result, if the AI-tree returns an empty result set for a particular query, a regular R-tree search is invoked to verify and resolve the case (see Figure 3).

#### IV. CHOICE OF ML MODELS



(b) An example of the custom loss function

For the binary classifier (i.e., overlap ratio classifier), the goal is to train an ML model to classify an incoming query as high- or low-overlap. We use a Random Forest classifier (RF, for short) [23] as the binary classifier. The prediction accuracy of the binary RF classifier is around 80% over different values of  $\alpha$ . Although, with proper training any binary classifier can be used in the AI+R-tree, the chosen RF classifier generalizes well across different datasets. As a result, in this paper, we do not vary the choice of ML models for this binary classification task. On the other hand, to investigate the impact of the chosen ML model on the average query recall, average query processing time, and average ML model size, we use three variants of Decision-Tree-based (DT, for short) [24], [25] classifiers, and two variants of a neural-network-based classifier. However, depending on the dataset at hand, any multi-label classifier [26] can be used to build the AI+R-tree.

##### A. The Binary Classifier

The steps to train the binary classifier are as follows: Assign Label 0 for queries where  $\alpha \leq \tau$  (e.g.,  $\alpha \leq 0.75$ ), and Label 1 for queries where  $\alpha > \tau$  (e.g.,  $\alpha > 0.75$ ). The training and test sets are split using an 80-20 ratio. The scikit-learn python library [27] is used for the RF classifier.

##### B. The Multi-label Classifier

1) *DT-based Classifiers*: We use three DT-based classifiers for the multi-label classification task: the basic Decision Tree (DCT, for short), RF, and XGBoost (XG, for short) [28].

2) *NN-based Classifier*: In the context of learned indexes, it is generally recommended to adopt a simple ML model (e.g., linear regression, decision tree) whenever possible [10]. However, it has been observed that a customized ML model tailored to the problem definition has the potential to achieve high performance compared to its basic counterpart. For example, in [29], a tailored regression model achieves high performance. Although neural-network-based models (NN-based models, for short) require longer training time, there is growing interest in designing NN-based ML models [30]–[32] for use in learned indexes. We investigate NN-based models as a multi-label classifier, and study their flexibility and the benefit of tailoring NN-based models for the AI+R-tree. We experiment



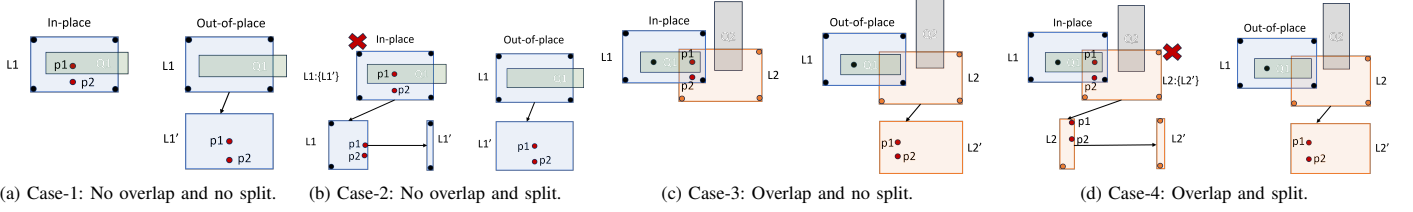


Fig. 7. In-place vs. Out-of-place insertion strategies

with two NN-based model variants based on the underlying loss function. We leverage a standard Binary Cross Entropy Loss function (BCELoss, for short) [33]. The BCELoss is used as a criterion to calculate the binary cross entropy between the input and the target probabilities. Then, we design a custom loss function for the AI+R-tree’s classification task.

Based on the problem formulation of the AI+R-tree, during the model training phase, given an input query, the multi-label classifier predicts a set of leaf node IDs. In the context of the multi-label NN-based classifier, the training and validation loss is calculated based on a pre-defined criterion (e.g., BCELoss). The standard BCELoss function takes two parameters as input: Model prediction and the ground truth. Notice that our goal is to maximize the average query recall in terms of number of retrieved data objects while reducing the number of false positive/negative predictions. However, the goal of maximizing the average query recall might not be fully captured by calculating the loss in terms of leaf node predictions only. For example, for an input range query, say  $Q$ , assume that the ground truth labels (i.e., leaf node ids) are:  $L1, L2, L3$ , and the number of qualifying data objects within  $L1, L2, L3$  (e.g., inside  $Q$ ) are 5, 10, 15, respectively. If an ML model predicts only  $L1$  correctly, the query recall is  $\frac{5}{30} = 0.16$ . On the other hand, if the same ML model predicts only  $L3$ , the query recall becomes  $\frac{15}{30} = 0.50$ . However, this information is not captured if we calculate the NN model loss in terms of leaf node predictions only. As a result, we design a custom loss function by including the information about the number of retrieved objects. The workflow of the custom loss function is given in Figure 6a.

In Figure 6b, we present an example to illustrate the process of the custom loss calculation. Consider an R-tree with two leaf nodes and four data objects. In Figure 6b, the given range query  $Q$  overlaps both leaf nodes. However, only Data Object-1 and Object-2 are contained inside the query rectangle. Notice that the custom loss function takes three parameters: model prediction, ground truth, and the R-tree. As we provide the R-tree as input to the custom loss function, we can build an  $m \times n$  matrix  $A$ , where  $m$  and  $n$  refer to the number of data objects and the number of leaf nodes, respectively. Although  $A$  can be a large matrix, the number of 1’s in a column of Matrix  $A$  is bounded by the maximum capacity of a leaf node. In other words, the total number of 1’s in  $A$  is exactly equal to  $m$ . Hence,  $A$  can be constructed and maintained efficiently as a sparse matrix. During training, we get the prediction of the model in terms of the predicted probabilities of the leaf node ids. We can treat the predictions as a vector, say  $x$ , and

generate the predicted probabilities in terms of retrieved data objects by performing the operation  $b = Ax$ . Notice that we can also create a similar ground truth vector in terms of data object (instead of leaf node ids). Finally, we can use a standard metric (e.g., binary cross entropy) to calculate the loss between the newly formulated prediction and the ground truth. In this paper, we refer to the NN-based models by BCE, and Custom loss functions by nnBCE and nnCustom, respectively. *Notice that the reason behind choosing the NN-based models is not to optimize for outperforming the other DT-based models but rather to show the potential benefit of designing a custom loss function tailored to the query processing requirements of the AI+R-tree.*

## V. DESIGN CHOICES FOR SUPPORTING INSERTS, UPDATES, AND DELETES

In the context of mutable (i.e., updateable) learned indexes, the two main strategies to support new data insertion are: In-place and Out-of-place (e.g., delta buffer) [10]. However, supporting inserts/updates comes at the cost of periodic re-organization (i.e., re-training) of the learned index structures or incorporating mechanisms that require additional space [10]. In this section, we present the design tradeoffs in adopting both In-place and Out-of-place strategies with the vision of realizing a mutable AI+R-tree.

### A. Supporting New Data Inserts

In the context of a mutable AI+R-tree, to avoid frequent ML model re-training, it is desirable to keep the R-tree component intact by deferring all structural modifications (whenever possible) for preserving the leaf node ID assignment as long as possible. Moreover, the correctness of the R-tree query processing should always be preserved to maintain the correctness of the AI+R-tree query processing. As a result, during the model re-training phase, the AI+R-tree can process all the incoming queries correctly using only the R-tree component. Hence, we advocate for using the R-tree component for new data inserts instead of using the AI-tree-based (i.e., ML-model-based) insert. We identify all the cases for supporting new data inserts using the R-tree component of the AI+R-tree. Moreover, for each of the cases, we present the design tradeoffs from the perspectives of both the AI-tree and the R-tree components, respectively.

We can identify two scenarios in the context of new data inserts into the R-tree component. In Scenario-1, the new data object is to be inserted into a leaf node and the leaf node does not overlap any other leaf node. Moreover, in Scenario-1, the

leaf node might (or might not) have space to accommodate the newly inserted object without (or with) invoking a node split operation. As a result, Scenario-1 leads to forming two cases. Case-1: No overlap and no split (Figure 7a), and Case-2: No overlap and split (Figure 7b). In Scenario-2, the new data object is to be inserted into a leaf node and the leaf node overlaps other leaf nodes. Moreover, in Scenario-2, the leaf node might (or might not) have space to accommodate the newly inserted object without (or with) invoking a node split operation. As a result, Scenario-2 leads to form two cases. Case-3: Overlap and no split (Figure 7c), and Case-4: Overlap and split (Figure 7d).

1) *Case-1*: In Figure 7a,  $L1$  and  $Q1$  represent a leaf node and a range query, respectively. New data points  $p1$  and  $p2$  are being inserted into  $L1$ . In Case-1, we assume that  $p1$  and  $p2$  can be inserted into  $L1$  without overflowing the leaf node, and there is no other leaf nodes overlapping  $L1$ . As a result, we refer to Case-1 as no-overlap-no-split. For the AI-tree component, if  $Q1$  is trained to predict the leaf node  $L1$ , it continues to do so for similar queries irrespective of the adopted insert strategy. Moreover, with an in-place strategy, only  $L1$  will be accessed. For an out-of-place strategy, both  $L1$  and  $L1'$  will be accessed. For the R-tree component, with an in-place strategy, only  $L1$  will be accessed. For an out-of-place strategy, both  $L1$  and  $L1'$  will be accessed. In Case-1, the in-place strategy potentially saves both space and time. However, the overlap ratio of  $Q1$  is impacted due to the in-place insert of point  $p1$ . As a result, the changes in overlap ratio of queries need to be considered in the re-training phase of the overlap ratio (i.e., the binary) classifier.

2) *Case-2*: In Figure 7b, we assume that  $L1$  overflows upon inserting  $p1$  and  $p2$ , and no other leaf nodes overlaps  $L1$ . As a result,  $L1$  will be split into  $L1$  and  $L1'$ . Hence, we refer to Case-2 as no-overlap-and-split. Moreover, with an in-place strategy, after the split, we assign the initial leaf node id  $L1$  to one of the newly created leaf nodes. Moreover, the other newly created leaf node is given the id  $L1'$ , and we maintain a link from  $L1$  to  $L1'$  as:  $L1 : \{L1'\}$ . In contrast, for out-of-place inserts, we defer the split to keep the leaf node ids intact as long as possible. Once  $L1$  reaches its maximum node capacity, an empty copy of  $L1$ , called  $L1'$ , will be created and will be linked to  $L1$ . Moreover, the new data points will be inserted into  $L1'$ . For the AI-tree component, if  $Q1$  is trained to predict the leaf node  $L1$ , it is maintained for similar queries irrespective of the adopted insert strategy. For both the in-place and out-of-place policies, the AI-tree needs to access both  $L1$  and  $L1'$  for processing  $Q1$ . Similarly, for the R-tree component, both in-place and out-of-place strategies require accessing both  $L1$  and  $L1'$ . In Case-2, there is no clear winner between the in-place and out-of-place insert strategies.

3) *Case-3*: In Figure 7c,  $L1$ ,  $L2$ , and  $Q1$ ,  $Q2$  represent leaf nodes and range queries, respectively. New data points  $p1$  and  $p2$  are being inserted into  $L2$ . In Case-3, we assume that there is an overlap between  $L1$  and  $L2$ , and  $p1$ ,  $p2$  can be inserted into  $L2$  without overflowing  $L2$ . As a result, we refer to Case-3 as overlap-and-no-split. For the AI-tree component, if  $Q1$  is trained to predict the leaf node  $L1$ , it continues for  $Q1$  and similar queries irrespective of the adopted insert strategy.

However, after the insert of  $p1$ ,  $p2$  with an in-place strategy, for processing  $Q1$ , the AI-tree does not predict  $L2$  until model re-training is performed. Hence, the AI-tree will not return  $p1$  until model re-training. On the other hand, if  $Q2$  is trained to predict none of  $L1$  and  $L2$ , the trained model is not impacted due to the new data inserts. In Case-3, adopting an out-of-place insert policy, the AI-tree processes  $Q1$  and  $Q2$  similar to the in-place strategy. For the R-tree component, after the inserts of  $p1$ ,  $p2$ , with an in-place strategy, the R-tree accesses both  $L1$ ,  $L2$  for processing  $Q1$ , and only  $L2$  for processing  $Q2$ . However, following an out-of-place strategy, the R-tree component accesses additional  $L2'$  for processing both  $Q1$  and  $Q2$ . In Case-3, the in-place strategy potentially saves both space and time for most of the queries. However, the overlap ratio of  $Q1$  is impacted due to the in-place insert of Point  $p1$  into  $L2$ . As a result, the changes in overlap ratio of queries need to be considered in the re-training phase of the overlap ratio classifier.

4) *Case-4*: In Figure 7d, we assume an overlap exists between  $L1$  and  $L2$ , and  $L2$  overflows upon inserts of  $p1$  and  $p2$ . Hence, we refer to Case-4 as overlap-and-split. Moreover, with an in-place strategy, after a split, we assign the initial leaf node id  $L2$  to one of the newly created leaf nodes. Moreover, the other newly created leaf node is given the id  $L2'$ , and we maintain a link from  $L2$  to  $L2'$  as:  $L2 : \{L2'\}$ . In contrast, for out-of-place inserts, we defer the split to keep the leaf node ids intact as long as possible. Once  $L2$  reaches its maximum node capacity, an empty copy of  $L2$  called  $L2'$  is created, and is linked to  $L2$ . Moreover, the new data points will be inserted into  $L2'$ . Similar to Case-3, in Case-4, the AI-tree component processes both  $Q1$  and  $Q2$  similarly irrespective of the adopted insert strategy. For the R-tree component, after inserting  $p1$ ,  $p2$ , with an in-place strategy, the R-tree accesses  $L2$ , and skips  $L2'$  (no overlap between  $Q1$  and the newly created  $L2'$ ) for processing  $Q1$ . However, for processing  $Q2$ , the R-tree does not access either  $L2$  or  $L2'$  due to the no overlap with  $Q2$ . In contrast, following an out-of-place strategy, the R-tree will have to access additionally  $L2'$  for processing both  $Q1$  and  $Q2$ . In Case-4, the in-place strategy potentially saves both space and time for certain queries (e.g.,  $Q2$ ) processed by the R-tree component.

## B. Supporting Deletes and Updates

In the AI+R-tree, a delete is supported by adopting any of the in-place or out-of-place strategies. However, we can avoid the cost of additional space by adopting an in-place delete strategy. Thus, a delete is treated as a logical operation by marking the data items deleted so that the marked items can be physically deleted at a later time. Hence, a logical delete can be performed in-place. Notice that the motivation behind performing a logical delete is to defer structural modification of leaf nodes until model re-training happens.

Updates are supported by performing a delete followed by an insert.

## C. Discussion

Here, we advocate for using the R-tree component for new data inserts instead of using the AI-tree-based (i.e., ML-

model-based) inserts. However, using the traditional R-tree component for inserts will bypass the AI-tree adaptation. Hence, the AI-tree component will not be aware of the newly inserted items until the ML models are re-trained. Notice that the performance of a mutable AI+R-tree adopting either the in-place or the out-of-place insert strategy is expected to be less impacted in both Cases-1 and-2. However, as illustrated in Cases-3 and-4, the performance of a mutable AI+R-tree can be negatively impacted until the ML models are re-trained. ML model re-training can be triggered periodically (e.g., based on a pre-defined performance deterioration threshold) to maintain high query processing performance. Otherwise, a separate data/workload distribution change detection mechanism can be employed to trigger the ML-model re-training phase [34]. Moreover, the AI+R-tree can fall back to the traditional R-tree component during the re-training process or in case of a significant distribution shift similar to the hybrid structure in [35]. As a future direction, we plan to investigate the query processing performance over a mutable AI+R-tree by adopting different insert strategies (see Section VIII).

## VI. EVALUATION

We run all experiments on an Ubuntu 18.04 with Intel Xeon Platinum 8168 (2.70GHz) and 3TB of total available memory.

### A. Datasets

We use three datasets from the UCR Spatio-Temporal Active Repository, namely UCR-STAR [36]. Specifically, we use three real-world datasets with two-dimensional location data (in the form of longitude and latitude). The Tweets location dataset contains the locations of real tweets, the Gowalla dataset contains the locations of users from a social networking website, and the Chicago crimes dataset contains the locations of Chicago crimes. Moreover, we preprocess the datasets to eliminate duplicate and missing values. For the Tweets locations dataset, we create a processed dataset containing the first 2 Million tweet locations. For the processed Gowalla and Chicago crimes datasets, there are 1.2 Million and 872, 127 records, respectively.

### B. The AI+R-tree Parameter Settings

1) *R-tree Parameters*: We construct the R-tree using a one-at-a-time tuple insert method to replicate the scenario of a dynamic environment. Moreover, we use a linear node-splitting algorithm for R-tree construction. On the other hand, due to the observed advantage of larger leaf node capacity in [18], we have set the maximum leaf capacity  $M = 1000$  for the R-tree. We fix the leaf node capacity for all experiments to observe the AI+R-tree performance by varying the ML model type.

2) *Query Selectivity and Values of  $\alpha$* : For a particular dataset, to demonstrate the query performance for a particular value of  $\alpha$ , 1000 synthetic range queries are used in the experiments with a fixed selectivity. For example, in the case of the Tweets locations dataset, a range query with Selectivity 0.00005 returns approximately 100 objects, a query

with Selectivity 0.0001 returns approximately 200 objects, and a query with Selectivity 0.0002 returns approximately 400 objects. In the experiments, the selectivity varies among  $[0.00005, 0.0001, 0.0002]$ . Moreover, we categorize the queries into five different values of  $\alpha$   $[0.1, 0.25, 0.5, 0.75, 1.0]$ . Thus, for each dataset, for all variations of selectivities and  $\alpha$  values, we use 15000 queries in total. Notice that all evaluations are performed by splitting each query set into 60%/20%/20% (train/validation/test), unless a specific split is specified.

3) *The AI-tree Parameters*: The AI-tree has two parameters: The size of the grid (see Section II-C) and the choice of the threshold  $\tau$  (see Figure 2). Similar to the process of hyperparameter tuning [22] for ML models, we start from a grid size  $2X2$ , and increase the size (e.g.,  $4X4$ ) to get the best fit for the validation data. As we vary the choices of ML models, the choices of the grid size also vary based on the type of the ML model. For example, the basic DT-based Model (referred to as DCT in the figures) performs well on the validation set for a grid with finer granularity:  $20X20$ . On the other hand, the ensemble methods, e.g., RF and XG, perform best for a grid with coarser granularity:  $4X4$ . Moreover, considering the training overhead, for the NN models, we do not vary the grid size but rather train a single NN model to demonstrate the benefit of the custom loss function. On the other hand, for a query  $Q$  with  $\alpha = 0.75$ , the  $\frac{TN(Q)}{VN(Q)}$  can be e.g.,  $\frac{15}{20}$ . Thus, there is room for improvement unless  $\alpha = 1$ . As a result, we set Threshold  $\tau = 0.75$ . In other words, for an incoming range query, if  $\alpha \leq 0.75$ , it is identified as a high-overlap query. If  $\alpha > 0.75$ , it is considered low-overlap.

### C. Implementation and Measurements

We realize the AI+R-tree using an open-source python library for the R-tree available on Github <sup>1</sup>. We integrate the AI+R-tree inside the library and run the experiments using Python version 3.6.9. On the other hand, for a disk-based R-tree index realized inside a practical system, the performance of a query depends on the number of leaf node accesses. In the experiments, we assume that the required number of disk I/Os is equivalent to the number of leaf node accesses [37]. For a query, we measure the CPU time, and count the number of leaf node accesses. Then, we multiply the number of leaf node accesses by a standard disk I/O access time. Finally, we sum the CPU and disk I/O times to report the average query processing time (in milliseconds). Notice that for a query workload with a particular selectivity, to demonstrate the performance for each value of  $\alpha$ , we run each experiment individually for each value of  $\alpha$ . This enables us to report the average query processing time, and the average query recall for each value of  $\alpha$ .

1) *ML Model Parameters*: For the DT-based ML models, we use the standard scikit-learn python library [27]. We use the default parameters for the DCT classifier. For the RF classifier, we have varied the  $n\_estimators$  parameter on the validation set, and picked the best value for testing. For

<sup>1</sup><https://github.com/sergkr/treelib>

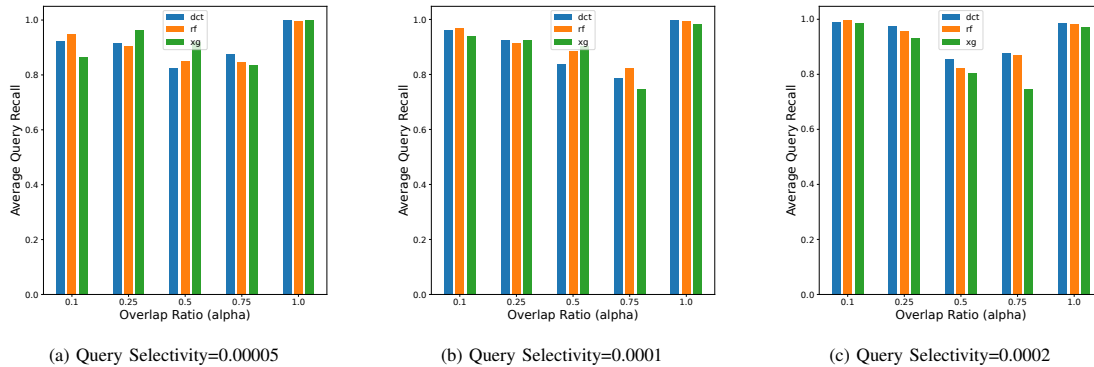


Fig. 8. Average query recall of DT based classifiers for the Tweets location dataset. The R-tree recall is always 1, hence is omitted in the figures.

the XG classifier, we have used the `xgboost`<sup>2</sup> library with default parameters for multi-label classification. For the NN-based classifiers, we implement a Multi Layer Perception (MLP) with three hidden layers and ReLU activation function using the standard `pytorch` [38] library. Moreover, we use the Adam [39] optimizer with learning rate  $10^{-3}$ , and train for 30 epochs to show the performance comparison between the `nnBCE` and `nnCustom` models.

#### D. Experimental Results

In each of the figures for each of the datasets, we show the value of overlap ratio  $\alpha$  in the X-axis and the average query processing time (in milliseconds) in the Y-axis. Moreover, we report the average query recall of the AI+R-tree for each type of ML model. Notice that the query recall for the traditional R-tree is always 1. Hence, the R-tree recall is omitted from the figures used for reporting query recall. On the other hand, the precision of the AI+R-tree is always 1 because the data objects of the predicted leaf nodes are checked against the query range.

##### 1) Effect of DT-based Models for the Tweet Location Dataset:

a) *Average Query Recall*: In Figure 8, we observe that the DT-based models maintain average query recall over 85% for high-overlap queries with overlap ratio in 0.10 and 0.25. For queries with selectivity 0.0002, the recall reaches up to 99%. However, for queries with overlap ratio closer to the threshold, the recall deteriorates for all variants of the DT-based model. Notice that the DT and RF classifiers perform better than the XG models for queries with overlap ratios between 0.50 and 0.75. For queries with  $\alpha = 1$ , the AI+R-tree processes most of the queries using its R-tree component. As a result, the recall almost reaches 1.

b) *Average Query Processing Time*: In Figure 9, we observe that the DT-based models maintains low query latency for processing high-overlap queries across all selectivities. Particularly, the DCT classifier enhances the query processing performance by up to 3.1X to 5.4X for queries with overlap ratio 0.10. Although the query processing time deteriorates for queries with overlap ratio closer to the threshold, it closely

follows the performance of a regular R-tree. Notice that the DCT classifier performs slightly better than the RF and XG models across all selectivities. For queries with  $\alpha = 1$ , the AI+R-tree processes most of the queries using its R-tree component. As a result, the query processing time almost matches the R-tree query processing time.

##### 2) Effect of Loss Functions of the NN Model for the Tweets Location Dataset:

a) *Average Query Recall*: In Figure 10, the average query recall is shown for each NN-based ML models for queries with various selectivities. The average query recall of both `nnBCE` and the `nnCustom` model are similar for the queries with very high alpha values (e.g., 0.10 and 0.25). However, the recall of the `nnBCE` model is higher in case of the queries with  $\alpha$  values in [0.50, 0.75].

b) *Average Query Processing Time*: In Figure 11, the average query processing time is shown for each NN-based ML models for queries with various selectivities. Although the average query recall of `nnBCE` is higher than that of `nnCustom`, the `nnCustom` model achieves this recall with significantly less query latency. The reason behind this performance gain is as follows. The `nnBCE` model predicts many false positives compared to the `nnCustom` model. As a result, the `nnBCE` model requires to search many extraneous leaf nodes compared to the `nnCustom` model. Moreover, the `nnCustom` model takes into account the benefit of predicting a leaf node with its contribution to the final result of the range queries. Notice that the goal of the experiments related to the NN-based models is to demonstrate the potential benefit of designing a loss function tailored to the requirements of the AI+R-tree query processing.

TABLE I  
AVERAGE ML MODEL SIZE OF THE AI+R-TREE FOR THE TWEETS LOCATION DATASET ACROSS ALL  $\alpha$  VALUES (IN MBS)

| Selectivity | R-tree  | DT-based models |      |      | NN-based models |          |
|-------------|---------|-----------------|------|------|-----------------|----------|
|             |         | DCT             | RF   | XG   | nnBCE           | nnCustom |
| 0.00005     | 1106.54 | 2.91            | 3.44 | 0.12 | 0.13            | 0.13     |
| 0.0001      | 1106.54 | 2.80            | 3.44 | 0.12 | 0.13            | 0.13     |
| 0.0002      | 1106.54 | 2.61            | 3.44 | 0.12 | 0.13            | 0.13     |

<sup>2</sup><https://xgboost.readthedocs.io/en/stable/tutorials/multioutput.html>



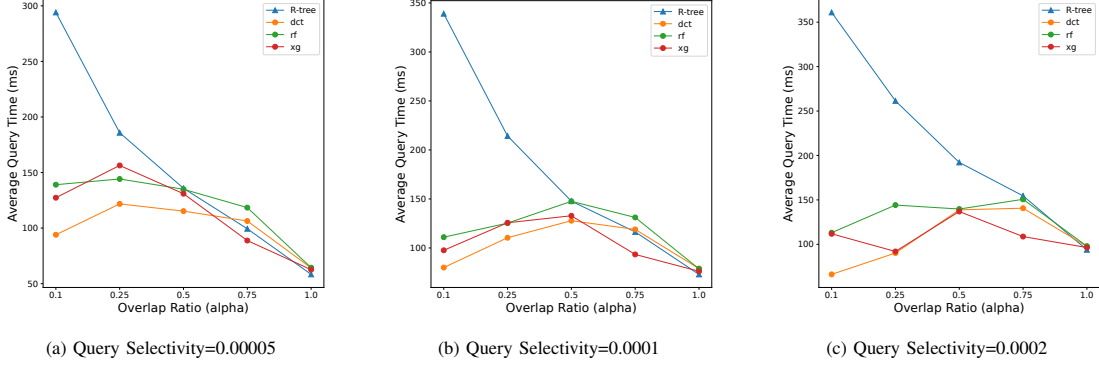


Fig. 9. Average query time of DT based classifiers for the Tweets dataset

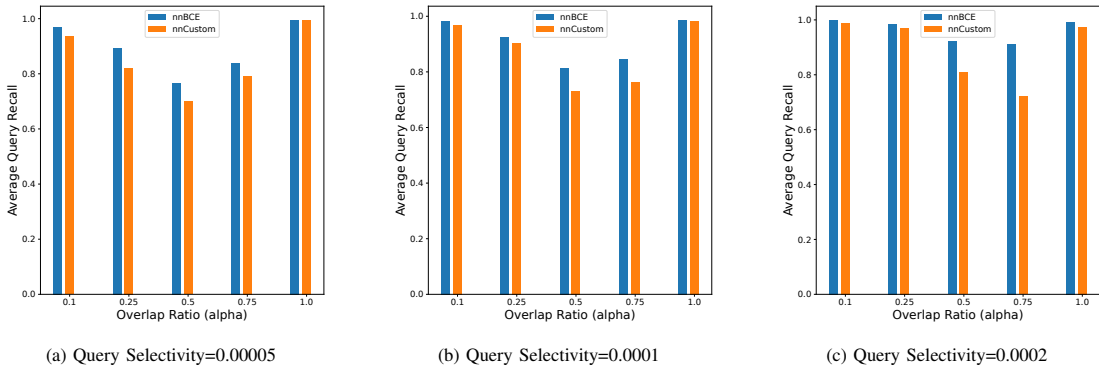


Fig. 10. Average query recall of NN based classifiers for the tweet locations dataset

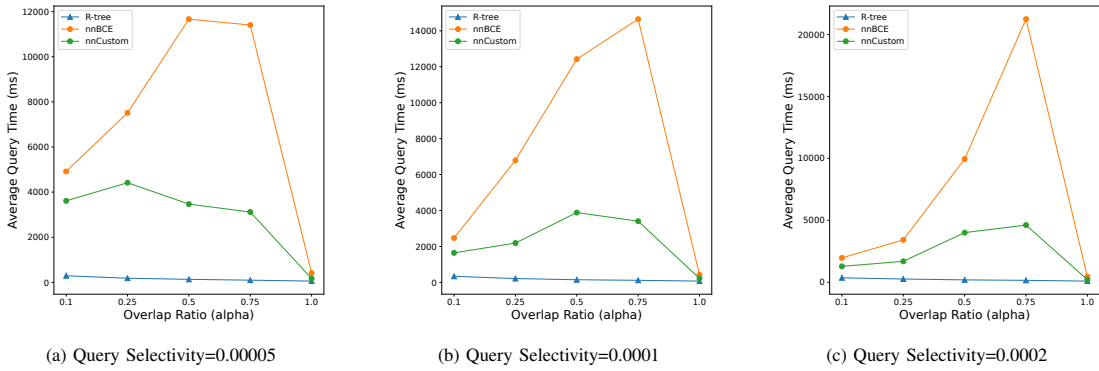


Fig. 11. Average query time of NN based classifiers for the tweet locations dataset

3) *Space Consumption of the ML Models for the Tweets Location Dataset:* In Table I, we present the R-tree size and the average ML model overhead across all  $\alpha$  values. Notice that the model size includes both the binary and the multi-label classifiers. For the Tweets location dataset, the model overhead varies between 0.01% to 0.26%. Notice that the space consumption of the NN-based model does not depend on the underlying loss function.

#### 4) Effect of DT-based Models for the Gowalla Dataset:

a) *Average Query Recall:* In Figure 12, we observe that the DT-based models maintain average query recall over 93% for high-overlap queries with overlap ratio in 0.10 and 0.25

across all selectivities. For the queries with selectivity 0.0002, the recall reaches up to 98%. However, similar to the Tweets location dataset, for queries with overlap ratio closer to the threshold, the recall deteriorates for all variants of the DT-based model.

b) *Average Query Processing Time:* In Figure 13, we observe that the DT-based models maintains low query latency for processing high-overlap queries across all selectivities. Particularly, the DCT classifier enhances the query processing performance by up to 3.2X to 4.7X for queries with overlap ratio 0.10.

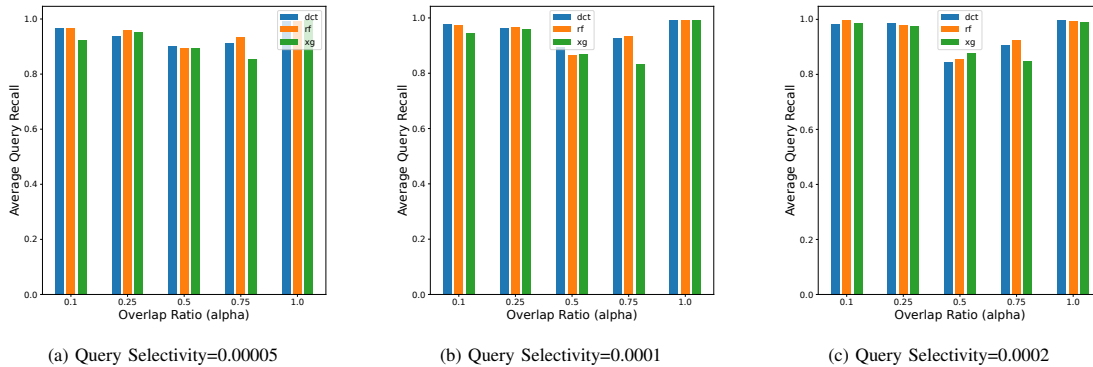


Fig. 12. Average query recall of DT based classifiers for the Gowalla dataset. The R-tree recall is always 1 and is not shown in the figures.

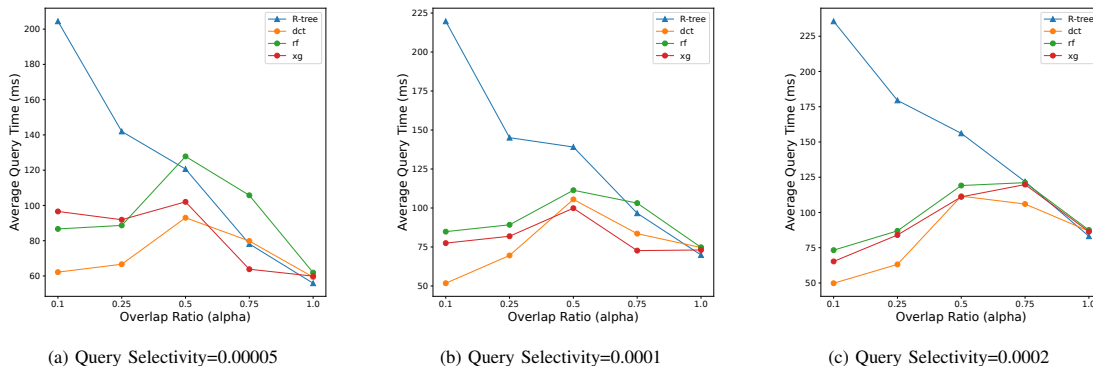


Fig. 13. Average query processing time of DT-based classifiers for the Gowalla dataset

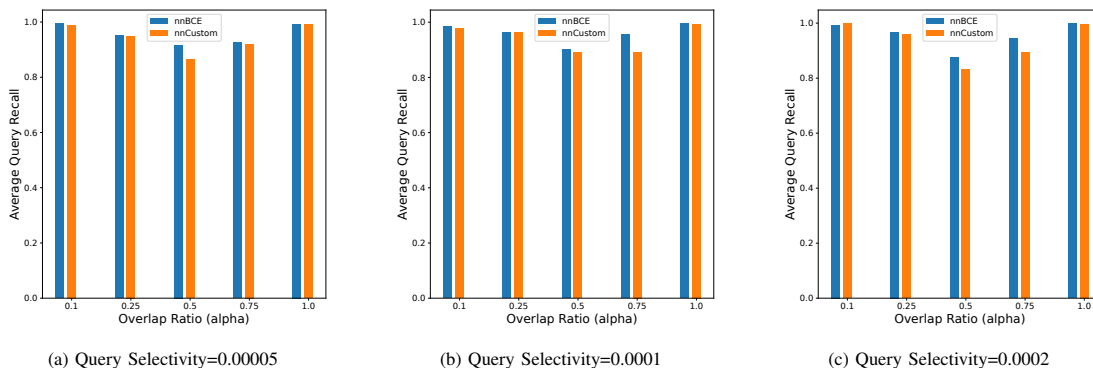


Fig. 14. Average query recall of NN based classifiers for the Gowalla dataset

### 5) Effect of Loss Functions of the NN Model for the Gowalla Dataset:

*a) Average Query Recall:* In Figure 14, we observe that the average query recall of both nnBCE and the nnCustom model are similar across all values of  $\alpha$ . However, similar to the Tweets location dataset, the nnBCE model achieves higher recall than that of the nnCustom model for some values of  $\alpha$ .

*b) Average Query Processing Time:* In Figure 15, the average query processing time is shown for each NN-based ML models for queries with various selectivities. Similar to the Tweets location dataset, the nnBCE models achieves higher recall with significant penalty on the query processing time.

On the other hand, the nnCustom model achieves similar recall with significantly less query latency.

TABLE II  
AVERAGE ML MODEL SIZE OF THE AI+R-TREE FOR THE GOWALLA DATASET ACROSS ALL  $\alpha$  VALUES (IN MBS)

| Selectivity | R-tree | DT based models |      |      | NN based models |          |
|-------------|--------|-----------------|------|------|-----------------|----------|
|             |        | DCT             | RF   | XG   | nnBCE           | nnCustom |
| 0.00005     | 695.61 | 9.30            | 4.18 | 0.11 | 0.13            | 0.13     |
| 0.0001      | 695.61 | 8.82            | 4.18 | 0.11 | 0.13            | 0.13     |
| 0.0002      | 695.61 | 7.62            | 4.18 | 0.11 | 0.13            | 0.13     |

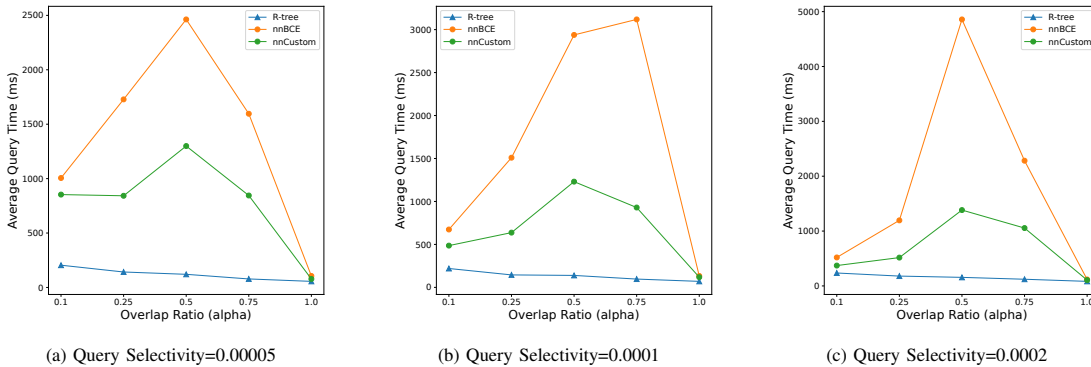


Fig. 15. Average query time of NN based classifiers for the Gowalla dataset

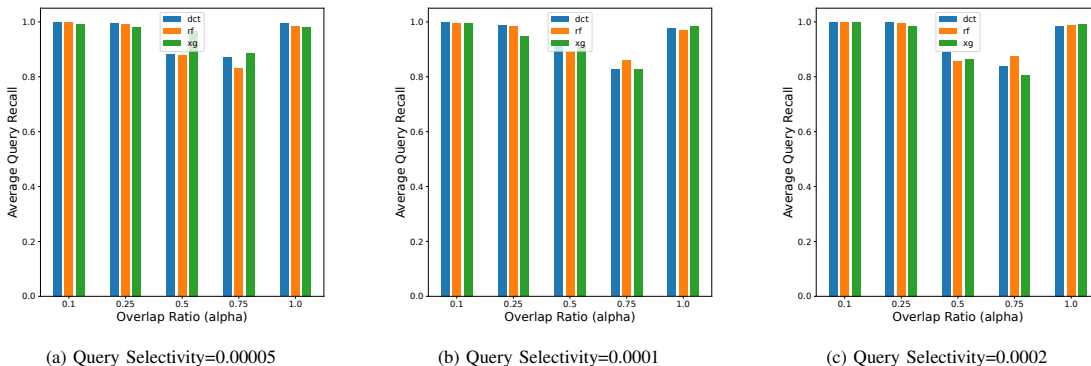


Fig. 16. Average query recall of DT-based classifiers for the Chicago Crimes dataset. The R-tree recall is always 1 and is not shown in the figures.

6) *Space Consumption of the ML Models for the Gowalla Dataset:* In Table II, we present the R-tree size and the average ML model overhead across all  $\alpha$  values. For the Gowalla dataset, the model overhead varies between 0.01% to 1.33%. Based on the query workload distribution, the DCT model normally requires a finer grid to create more decision trees than the RF and XG models. As a result, the DCT model consumes more space than the other model type for the Gowalla dataset.

7) *Effect of DT-based Models for the Chicago Crimes Dataset:*

a) *Average Query Recall:* In Figure 16, we observe that the DT-based models maintain average query recall over 98% for high-overlap queries with overlap ratio in 0.10 and 0.25 across all selectivities. For the queries with selectivity 0.0002, the recall reaches up to 99%. However, similar to the Tweets location and Gowalla datasets, for queries with overlap ratio closer to the threshold, the recall deteriorates for all variants of the DT-based model.

b) *Average Query Processing Time:* In Figure 17, we observe that the DT-based models maintain low query latency for processing high-overlap queries across all selectivities. Particularly, the DCT classifier enhances the query processing performance by up to 2.6X to 5.2X for queries with overlap ratio 0.10.

8) *Effect of Loss Functions of the NN Model for the Chicago Crimes Dataset:*

a) *Average Query Recall:* In Figure 18, we observe that the average query recall of both nnBCE and the nnCustom

model are similar across all values of  $\alpha$ . However, similar to the Tweets location and Gowalla datasets, the nnBCE model achieves higher recall than the nnCustom model for some values of  $\alpha$ .

b) *Average Query Processing Time:* In Figure 19, similar to the Tweets location and Gowalla datasets, we observe that the nnBCE models achieve higher recall with significant penalty on the query processing time. On the other hand, the nnCustom model achieves similar recall with significantly less query latency.

TABLE III  
AVERAGE ML MODEL SIZE OF THE AI+R-TREE FOR THE CHICAGO CRIMES DATASET ACROSS ALL  $\alpha$  VALUES (IN MBs)

| Selectivity | R-tree | DT-based models |      |      | NN-based models |          |
|-------------|--------|-----------------|------|------|-----------------|----------|
|             |        | DCT             | RF   | XG   | nnBCE           | nnCustom |
| 0.00005     | 482.64 | 0.94            | 1.60 | 0.11 | 0.13            | 0.13     |
| 0.0001      | 482.64 | 0.94            | 1.61 | 0.11 | 0.13            | 0.13     |
| 0.0002      | 482.64 | 0.94            | 1.61 | 0.11 | 0.13            | 0.13     |

9) *Space Consumption of the ML Models for the Chicago Crimes Dataset:* In Table III, we present the R-tree size and the average ML model overhead across all  $\alpha$  values. Notice that the model size includes both the binary and the multi-label classifiers. For the Chicago Crimes dataset, the model overhead varies between 0.02% to 0.33%.

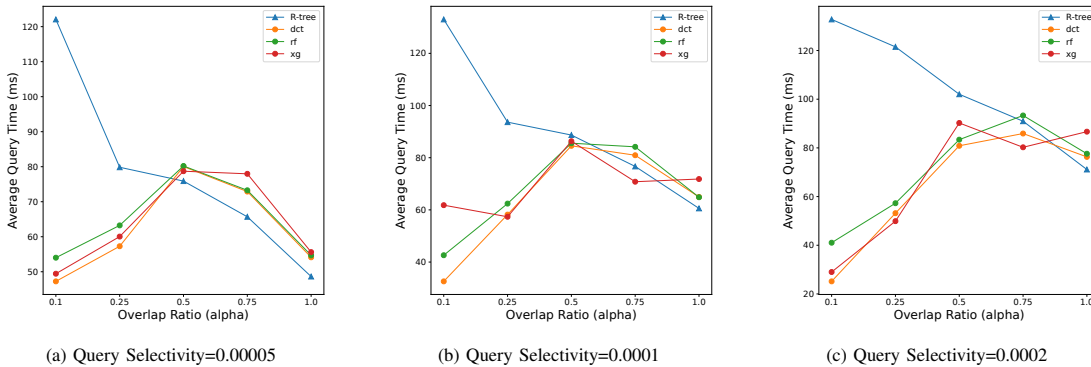


Fig. 17. Average query time of DT-based classifiers for the Chicago Crimes dataset

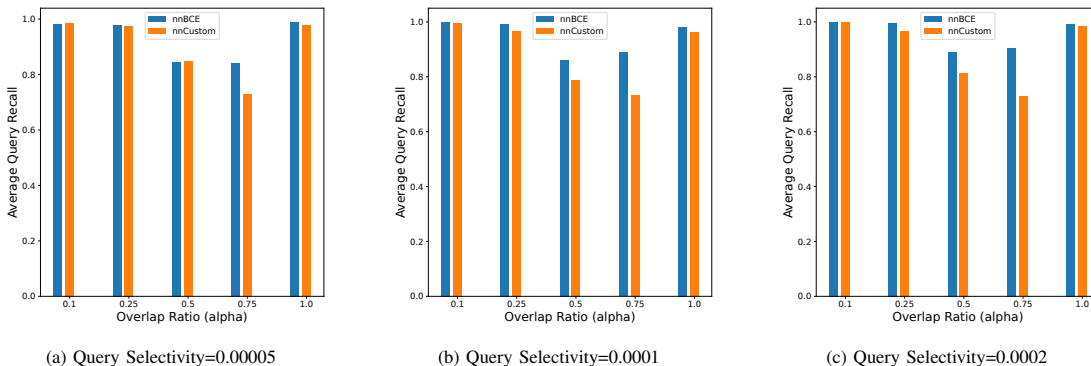


Fig. 18. Average query recall of NN based classifiers for the Chicago Crimes dataset

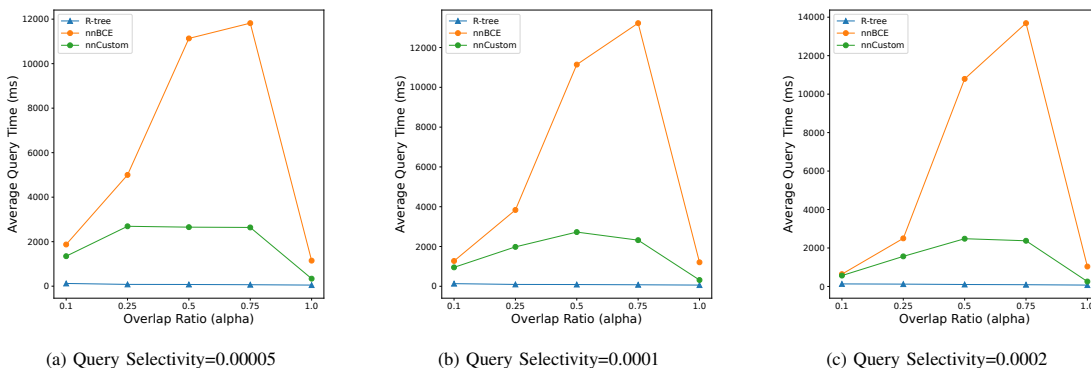


Fig. 19. Average query time of NN based classifiers for the Chicago Crimes dataset

## VII. RELATED WORK

Many variants of the R-tree exist, e.g., see [13], [15], [40]–[46]. On the other hand, in the context of learned multi-dimensional and spatial indexes, there are several variants of ML-enhanced R-trees, e.g., [47]–[49]. In [47]–[49], the goal is to leverage ML techniques to build a better R-tree to replace the traditional heuristic presented in the index construction algorithm (e.g., choosing sub-tree during new data insertions). As a result, the query processing performance is expected to be improved. Moreover, these ML-enhanced variants of R-trees do not modify the query processing algorithms but rather advocate for re-using the existing query processing

techniques. Notice that regardless of the type of the R-tree, all R-tree variants attempt to reduce the amount of node overlap. However, with dynamic updates, the shape of a constructed R-tree deteriorates. As a result, our design principles for the AI+R-tree can be applied to any of the R-tree variants.

A class of learned multi-dimensional indexes is designed to replace a traditional multi-dimensional index structure [7]–[10]. However, in the context of the AI+R-tree, our target is not to replace the existing index structure rather to enhance its performance using ML models. On the other hand, there are several learned multi-dimensional indexes that leverage a projection function to map the multi-dimensional points

into one-dimension [7]–[10]. After that any one-dimensional learned index can be used in the projected space. However, the proposed AI+R-tree avoids using a projection function, and operate directly on the original multi-dimensional representation of the spatial data objects.

The idea of using helper ML models inside traditional multi-dimensional and spatial indexes to enhance their query processing performance has been presented in [50]–[52]. In the context of ML-enhanced multi-dimensional indexes, the focus of the above mentioned techniques is not on analyzing (i.e., high- vs. low-overlap queries) and optimizing the index for the given query workload. Notice that the AI+R-tree focuses on analyzing the query workload to identify the queries for which a traditional disk-based spatial index (in this case, the R-tree) does not perform well. Moreover, we propose to adopt a hybrid approach to leverage the benefit of both the proposed AI-tree, and the traditional R-tree.

The tradeoffs between In-place and Out-of-place strategies for supporting updates in the context of learned one-dimensional indexes have been identified in [53]. In contrast, in this paper, we present the design tradeoffs for supporting both In-place and Out-of-place strategies in the context of the (learned multi-dimensional) AI+R-tree. On the other hand, the benefit of designing a custom loss function in the context of Space Partitioning has been presented in [54]. In this paper, we present a case study by identifying the potential benefit of designing a custom loss function in the context of the (learned multi-dimensional) AI+R-tree.

## VIII. FUTURE RESEARCH DIRECTIONS

### A. Investigating the Benefit of the Hybrid AI+X-tree Structure

Similar to the hybrid structure [35], the AI+R-tree can fall back to the traditional R-tree during the re-training process or in case of a significant distribution shift. Moreover, the benefit of a 2-tree architecture in the context of larger than memory indexes has been presented in [55]. Although the motivation and application of the proposed index in [55] is different than the AI+R-tree, the hybrid 2-tree (i.e., the AI-tree and R-tree) design of the AI+R-tree structure might be beneficial for other index structures as long as node overlaps exist, and hence multiple tree paths are explored during search. As a result, it is an interesting direction to investigate the benefit of the AI+X-tree structure, where  $X$  is a traditional spatial or a multi-dimensional index structure (e.g., the SS-tree [56]).

### B. Efficient Query Processing over the Mutable AI+R-tree

We have presented the design tradeoffs for realizing a mutable AI+R-tree. As a result, analyzing the empirical tradeoffs of the mutable AI+R-tree, and developing efficient query processing techniques over the mutable structure are interesting directions for future research. Moreover, incorporating the concept of Machine Unlearning [57] in the context of the mutable AI+R-tree is an interesting future research direction.

### C. Efficient Multi-label NN-based Classifier

An NN-based model provides an opportunity to design custom loss functions tailored to the requirement of the underlying learning task [54]. The proposed NN-based custom loss function shows promising results over the standard loss function. However, the query processing performance of the NN-based models is inferior to the DT-based models in the context of the AI+R-tree. As a result, based on the proposed custom loss function, investigating the techniques to develop an efficient multi-label NN-based classifier in the context of the AI+R-tree is an interesting direction for future research.

## IX. CONCLUSION

We investigate the empirical tradeoffs in processing dynamic query workloads over the AI+R-tree. Particularly, we investigate the impact of the choice of ML models on the AI+R-tree query processing performance. We present a case study of designing a custom loss function for a neural-network-based model tailored to the requirement of the AI+R-tree query processing. Furthermore, we present the design tradeoffs for supporting inserts/updates/deletes with the vision of realizing a mutable AI+R-tree. Experiments demonstrate that the AI+R-tree can maintain high recall and low query latency while processing dynamic query workloads. In summary, this paper takes an important step towards realizing the AI+R-tree in various practical settings, and opens several directions for future research within ML-enhanced R-tree structures.

## ACKNOWLEDGMENTS

The authors thank Dr. Raymond Yeh for his valuable discussion and feedback during the initial stages of this work. Jianguo Wang acknowledges the support of the National Science Foundation under Grant Number 2337806.

## REFERENCES

- [1] G. Cong, J. Yang, and Y. Zhao, “Machine learning for databases: Foundations, paradigms, and open problems,” in *Companion of the 2024 International Conference on Management of Data*, 2024, pp. 622–629.
- [2] T. Kraska, A. Beutel, E. H. Chi, J. Dean, and N. Polyzotis, “The case for learned index structures,” in *Proceedings of the ACM SIGMOD International Conference on Management of Data*, 2018, pp. 489–504.
- [3] P. Ferragina and G. Vinciguerra, “The pgm-index,” in *Proceedings of the VLDB Endowment*, 2020, p. 1162–1175.
- [4] J. Ding, U. F. Minhas, J. Yu, C. Wang, J. Do, Y. Li, H. Zhang, B. Chandramouli, J. Gehrke, D. Kossmann *et al.*, “Alex: an updatable adaptive learned index,” in *Proceedings of the ACM SIGMOD International Conference on Management of Data*, 2020, pp. 969–984.
- [5] J. Wu, Y. Zhang, S. Chen, J. Wang, Y. Chen, and C. Xing, “Updatable learned index with precise positions,” *Proc. VLDB Endow.*, vol. 14, no. 8, p. 1276–1288, apr 2021.
- [6] T. Kraska, M. Alizadeh, A. Beutel, E. H. Chi, J. Ding, A. Kristo, G. Leclerc, S. Madden, H. Mao, and V. Nathan, “Sagedb: A learned database system,” in *9th Biennial Conference on Innovative Data Systems Research*, 2019.
- [7] A. Al-Mamun, H. Wu, and W. G. Aref, “A tutorial on learned multi-dimensional indexes,” in *Proceedings of the 28th ACM SIGSPATIAL International Conference on Advances in Geographic Information Systems*, 2020, pp. 1–4.
- [8] Q. Liu, M. Li, Y. Zeng, Y. Shen, and L. Chen, “How good are multi-dimensional learned indices? an experimental survey,” *arXiv preprint arXiv:2405.05536*, 2024.
- [9] M. Li, H. Wang, H. Dai, M. Li, R. Gu, F. Chen, Z. Chen, S. Li, Q. Liu, and G. Chen, “A survey of multi-dimensional indexes: Past and future trends,” *IEEE Transactions on Knowledge and Data Engineering*, 2024.



- [10] A. Al-Mamun, H. Wu, Q. He, J. Wang, and W. G. Aref, "A survey of learned indexes for the multi-dimensional space," *arXiv preprint arXiv:2403.06456*, 2024.
- [11] A. Llavesh, U. Sirin, R. West, and A. Ailamaki, "Accelerating b+ tree search by using simple machine learning techniques," in *Proceedings of the 1st International Workshop on Applied AI for Database Systems and Applications*, 2019.
- [12] Y. Dai, Y. Xu, A. Ganesan, R. Alagappan, B. Kroth, A. Arpaci-Dusseau, and R. Arpaci-Dusseau, "From wiskey to bourbon: A learned index for log-structured merge trees," in *14th Symposium on Operating Systems Design and Implementation*, 2020, pp. 155–171.
- [13] A. Guttman, "R-trees: A dynamic index structure for spatial searching," in *Proceedings of the ACM SIGMOD international conference on Management of data*, 1984, pp. 47–57.
- [14] D. Comer, "Ubiquitous b-tree," *ACM Computing Surveys (CSUR)*, vol. 11, no. 2, pp. 121–137, 1979.
- [15] Y. Manolopoulos, A. Nanopoulos, A. N. Papadopoulos, and Y. Theodoridis, *R-trees: Theory and Applications*. Springer Science & Business Media, 2010.
- [16] P. Li, H. Lu, Q. Zheng, L. Yang, and G. Pan, "Lisa: A learned index structure for spatial data," *Proceedings of the ACM SIGMOD International Conference on Management of Data*, 2020.
- [17] F. Herrera, F. Charte, A. J. Rivera, and M. J. Del Jesus, "Multilabel classification," in *Multilabel Classification*. Springer, 2016, pp. 17–31.
- [18] A. Al-Mamun, C. M. R. Haider, J. Wang, and W. G. Aref, "The 'ai + r' - tree: An instance-optimized r - tree," in *2022 23rd IEEE International Conference on Mobile Data Management (MDM)*, 2022, pp. 9–18.
- [19] C. C. Aggarwal, "Data classification," in *Data Mining*. Springer, 2015, pp. 285–344.
- [20] W. Aref, D. Barbará, and P. Vallabhaneni, "The handwritten trie: Indexing electronic ink," in *SIGMOD Rec.*, 1995, p. 151–162.
- [21] C. M. Bishop and H. Bishop, *Deep learning: Foundations and concepts*. Springer Nature, 2023.
- [22] J. Bergstra, R. Bardenet, Y. Bengio, and B. Kégl, "Algorithms for hyperparameter optimization," *Advances in neural information processing systems*, vol. 24, 2011.
- [23] L. Breiman, "Random forests," *Machine learning*, vol. 45, no. 1, pp. 5–32, 2001.
- [24] E. Gibaja and S. Ventura, "A tutorial on multilabel learning," *ACM Computing Surveys (CSUR)*, vol. 47, no. 3, pp. 1–38, 2015.
- [25] J. R. Quinlan, "Induction of decision trees," *Machine learning*, vol. 1, no. 1, pp. 81–106, 1986.
- [26] P. Szymanski and T. Kajdanowicz, "Scikit-multilearn: a scikit-based python environment for performing multi-label classification," *The Journal of Machine Learning Research*, vol. 20, no. 1, pp. 209–230, 2019.
- [27] F. Pedregosa, G. Varoquaux, A. Gramfort, V. Michel, B. Thirion, O. Grisel, M. Blondel, P. Prettenhofer, R. Weiss, V. Dubourg, J. Vanderplas, A. Passos, D. Cournapeau, M. Brucher, M. Perrot, and E. Duchesnay, "Scikit-learn: Machine learning in Python," *Journal of Machine Learning Research*, vol. 12, pp. 2825–2830, 2011.
- [28] T. Chen and C. Guestrin, "Xgboost: A scalable tree boosting system," in *Proceedings of the 22nd acm sigkdd international conference on knowledge discovery and data mining*, 2016, pp. 785–794.
- [29] M. Eppert, P. Fent, and T. Neumann, "A tailored regression for learned indexes: Logarithmic error regression," in *Fourth Workshop in Exploiting AI Techniques for Data Management*, 2021, pp. 9–15.
- [30] D. Amato, G. L. Bosco, and R. Giancarlo, "On the suitability of neural networks as building blocks for the design of efficient learned indexes," in *International Conference on Engineering Applications of Neural Networks*. Springer, 2022, pp. 115–127.
- [31] D. Amato, G. Lo Bosco, and R. Giancarlo, "Neural networks as building blocks for the design of efficient learned indexes," *Neural Computing and Applications*, vol. 35, no. 29, pp. 21 399–21 414, 2023.
- [32] P. Ferragina, M. Frasca, G. C. Marinò, and G. Vinciguerra, "On nonlinear learned string indexing," *IEEE Access*, 2023.
- [33] "Pytorch module for loss functions." Accessed in 2024. [Online]. Available: <https://pytorch.org/docs/stable/generated/torch.nn.BCELoss.html>
- [34] V. Nathan, J. Ding, M. Alizadeh, and T. Kraska, "Learning multi-dimensional indexes," in *Proceedings of the ACM SIGMOD International Conference on Management of Data*, 2020, pp. 985–1000.
- [35] A. Davitkova, D. Gjurovski, and S. Michel, "Learning over sets for databases," *International Conference on Extending Database Technology (EDBT)*, 2024.
- [36] S. Ghosh, T. Vu, M. A. Eskandari, and A. Eldawy, "Ucr-star: The ucr spatio-temporal active repository," *SIGSPATIAL Special*, vol. 11, no. 2, pp. 34–40, 2019.
- [37] A. R. Mahmood, W. G. Aref, A. M. Aly, and S. Basalamah, "Indexing recent trajectories of moving objects," in *Proceedings of the 22nd ACM SIGSPATIAL International Conference on Advances in Geographic Information Systems*, 2014, pp. 393–396.
- [38] A. Paszke, S. Gross, F. Massa, A. Lerer, J. Bradbury, G. Chanan, T. Killeen, Z. Lin, N. Gimelshein, L. Antiga et al., "Pytorch: An imperative style, high-performance deep learning library," *Advances in neural information processing systems*, vol. 32, 2019.
- [39] D. P. Kingma, "Adam: A method for stochastic optimization," *arXiv preprint arXiv:1412.6980*, 2014.
- [40] T. Sellis, N. Roussopoulos, and C. Faloutsos, "The r+-tree: A dynamic index for multi-dimensional objects." Tech. Rep., 1987.
- [41] N. Beckmann, H.-P. Kriegel, R. Schneider, and B. Seeger, "The r\*-tree: an efficient and robust access method for points and rectangles," in *Proceedings of the ACM SIGMOD international conference on Management of data*, 1990, pp. 322–331.
- [42] N. Beckmann and B. Seeger, "A revised r\*-tree in comparison with related index structures," in *Proceedings of the ACM SIGMOD International Conference on Management of data*, 2009, pp. 799–812.
- [43] H. Samet, *Foundations of multidimensional and metric data structures*. Morgan Kaufmann, 2006.
- [44] D. Sidlauskas, S. Chester, E. T. Zacharatos, and A. Ailamaki, "Improving spatial data processing by clipping minimum bounding boxes," in *34th International Conference on Data Engineering (ICDE)*. IEEE, 2018, pp. 425–436.
- [45] L. Arge, M. D. Berg, H. Haverkort, and K. Yi, "The priority r-tree: A practically efficient and worst-case optimal r-tree," *ACM Transactions on Algorithms (TALG)*, vol. 4, no. 1, pp. 1–30, 2008.
- [46] I. Kamel and C. Faloutsos, "Hilbert r-tree: An improved r-tree using fractals," in *Proceedings of the 20th International Conference on Very Large Data Bases*, 1994, p. 500–509.
- [47] T. Gu, K. Feng, G. Cong, C. Long, Z. Wang, and S. Wang, "The rlr-tree: A reinforcement learning based r-tree for spatial data," *arXiv preprint arXiv:2103.04541*, 2021.
- [48] J. Yang and G. Cong, "Platon: Top-down r-tree packing with learned partition policy," *Proceedings of the ACM on Management of Data*, vol. 1, no. 4, pp. 1–26, 2023.
- [49] S. Huang, Y. Wang, and G. Li, "Acr-tree: Constructing r-trees using deep reinforcement learning," in *International Conference on Database Systems for Advanced Applications*. Springer, 2023, pp. 80–96.
- [50] A. Hadian, A. Kumar, and T. Heinis, "Hands-off model integration in spatial index structures," in *Proceedings of the 2nd International Workshop on Applied AI for Database Systems and Applications*, 2020.
- [51] V. Pandey, A. van Renen, A. Kipf, I. Sabek, J. Ding, and A. Kemper, "The case for learned spatial indexes," *arXiv preprint arXiv:2008.10349*, 2020.
- [52] R. Kang, W. Wu, C. Wang, C. Zhang, and J. Wang, "The case for ml-enhanced high-dimensional indexes," in *Proceedings of the 3rd International Workshop on Applied AI for Database Systems and Applications*, 2021.
- [53] S. Chatterjee, M. F. Pekala, L. Kruglyak, and S. Idreos, "Limousine: Blending learned and classical indexes to self-design larger-than-memory cloud storage engines," *Proceedings of the ACM on Management of Data*, vol. 2, no. 1, pp. 1–28, 2024.
- [54] A. Fahim, M. E. Ali, and M. A. Cheema, "Unsupervised space partitioning for nearest neighbor search," *International Conference on Extending Database Technology (EDBT)*, 2023.
- [55] X. Zhou, X. Yu, G. Graefe, and M. Stonebraker, "Two is better than one: The case for 2-tree for skewed data sets," *CIDR*, vol. 11, p. 13, 2023.
- [56] D. A. White and R. Jain, "Similarity indexing with the ss-tree," in *Proceedings of the Twelfth International Conference on Data Engineering*. IEEE, 1996, pp. 516–523.
- [57] M. Kurmanji, E. Triantafyllou, and P. Triantafyllou, "Machine unlearning in learned databases: An experimental analysis," *Proceedings of the ACM on Management of Data*, vol. 2, no. 1, pp. 1–26, 2024.

## X. BIOGRAPHY SECTION

**Abdullah-Al-Mamun** is a PhD candidate at the Department of Computer Science, Purdue University. His research interest is in the area of Machine Learning for Database Systems, particularly, in the field of Learned Multi- and High-dimensional Index Structures.

**Ch. Md. Rakin Haider** is a PhD candidate at the Department of Computer Science, Purdue University. His research interests are in the area of improving traditional systems using machine learning tools while maintaining certain desirable properties such as fairness and efficiency.

**Jianguo Wang** is a tenure-track assistant professor in the Department of Computer Science at Purdue University. He received his Ph.D. degree in Computer Science from UC San Diego. His research interests include disaggregated databases and vector databases. His research has won multiple prestigious awards, including the NSF CAREER Award and the SIGMOD Research Highlight Award.

**Walid G. Aref** is a professor of Computer Science at Purdue University. His research focus is in extending the functionality of database systems in support of emerging applications, e.g., spatial, spatio-temporal and graph databases. He is also interested in query processing, indexing, and data streaming. He has served as Editor-in-Chief of the ACM Transactions of Spatial Algorithms and Systems (ACM TSAS), associate editor of the VLDB Journal and the ACM Transactions of Database Systems (ACM TODS). Walid has won several best paper awards including the 2016 VLDB ten-year best paper award. He is a Fellow of the IEEE, and a member of the ACM.